Catalysis in a teacup, inspired by nature …

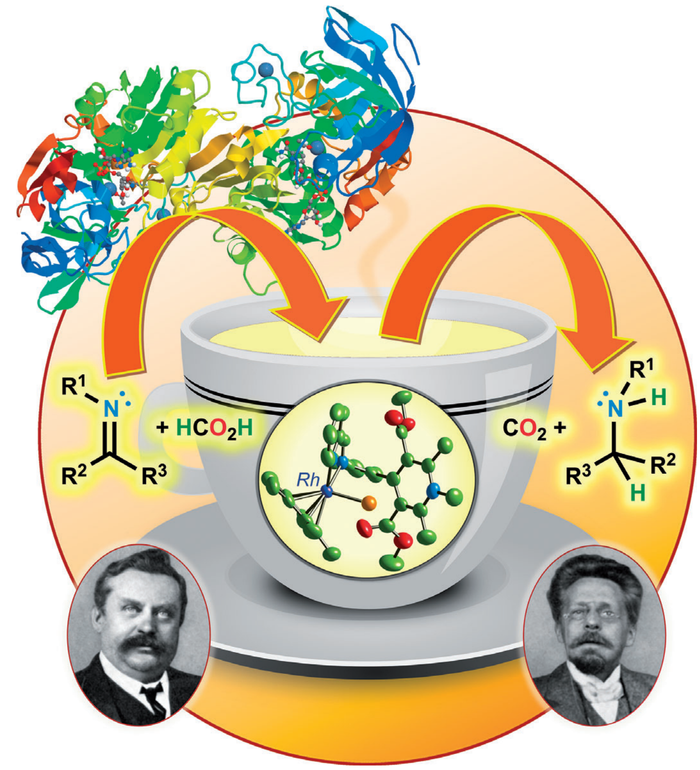

… Alfred Werner (left) received the 1913 Nobel Prize for his coordination theory of transition metal compounds, and Arthur Hantzsch (right) discovered the route to (dihydro)pyridines that bear his name. In their Communication on page 3411 ff., S. B. Colbran et al. disclose that conjugation of rhodium and Hantzsch pyridine centers affords a catalyst for the transfer hydrogenation of imines in air under ambient conditions. A key step in the catalysis mimics that in metallo-(de)hydrogenase enzymes.

Detecting DNA Damage

Cisplatin is a widely used cancer drug but its effect on cells is still not fully understood. In their Communication on page 3350 ff., U. Bierbach et al. describe a strategy for labeling anticancer platinum agents in cells.

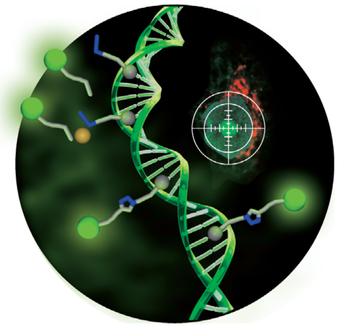

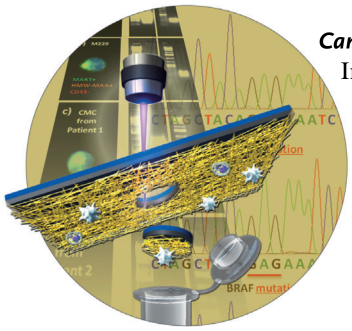

Cancer Cell Detection

In their Communication on page 3379 ff., M. A. Garcia, A. Ribas, R. S. Lo, H.-R. Tseng, et al. combine a polymer-nanofiber membrane with laser microdissection, for excising the cells of interest. Single cells can go on to be genotyped for cancer markers.

Trifluoromethylthiolation

In their Communication on page 3457 ff., L. Lu, Q. Shen, and co-workers reveal a new electrophilic hypervalent iodine reagent that reacts with a wide range of substrates under mild conditions.

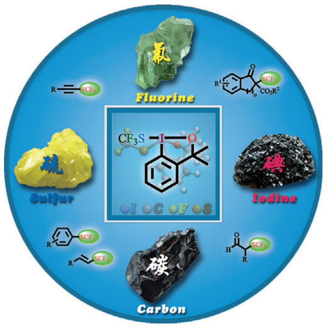

How to contact us:

Editorial Office:
E-mail: angewandte@wiley-vch.de
Fax: (+49) 6201–606-331
Telephone: (+49) 6201–606-315

Reprints, E-Prints, Posters, Calendars:
Carmen Leitner
E-mail: chem-reprints@wiley-vch.de
Fax: (+49) 6201–606-331
Telephone: (+49) 6201–606-327

Copyright Permission:
Bettina Loycke
E-mail: rights-and-licences@wiley-vch.de
Fax: (+49) 6201–606-332
Telephone: (+49) 6201–606-280

Online Open:
Margitta Schmitt, Carmen Leitner
E-mail: angewandte@wiley-vch.de
Fax: (+49) 6201–606-331
Telephone: (+49) 6201–606-315

Subscriptions:
www.wileycustomerhelp.com
Fax: (+49) 6201–606-184
Telephone: 0800 1800536 (Germany only)
+44(0) 1865476721 (all other countries)

Advertising:
Marion Schulz
E-mail: mschulz@wiley-vch.de
jspiess@wiley-vch.de
Fax: (+49) 6201–606-550
Telephone: (+49) 6201–606-565

Courier Services:
Boschstrasse 12, 69469 Weinheim

Regular Mail:
Postfach 101161, 69451 Weinheim

Angewandte Chemie International Edition is a journal of the Gesellschaft Deutscher Chemiker (GDCh), the largest chemistry-related scientific society in continental Europe. Information on the various activities and services of the GDCh, for example, cheaper subscription to *Angewandte Chemie International Edition*, as well as applications for membership can be found at **www.gdch.de** or can be requested from GDCh, Postfach 900440, D-60444 Frankfurt am Main, Germany.

GDCh
GESELLSCHAFT
DEUTSCHER CHEMIKER

Service

Author Profile

"My motto is 'full speed ahead.'
My favorite molecule is fluorine …"
This and more about Jean'ne M. Shreeve can be found on page 3308.

News

M. Shibasaki

C. V. Robinson

S. E. Gibson

J. K. Edwards

O.S. Wolfbeis

T. Carell

K. Matyjaszewski

Books

Highlights

Self-Assembly

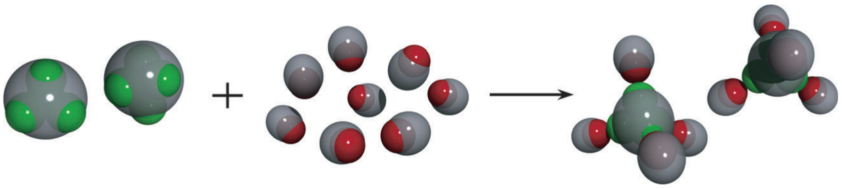

Sticking together: Colloidal particles with a determined number of sticky sites arranged in precise geometries analogous to atoms were created. The kinetics of the colloidal assemblies related to specific chemical reactions (see figure) were investigated using optical microscopy. This general method should allow for a broad range of useful 3D colloidal assemblies.

Asymmetric Catalysis

Chiral possibilities (Cp): In two approaches for introducing chirality into reactions of half-sandwich Rh complexes, dihydroisoquinolones have been synthesized from benzamides and olefins. In one approach C_2-symmetric Cp ligands were utilized, while in the other an artificial metalloenzyme was employed as the chiral catalyst, leading to high levels of enantioselectivity.

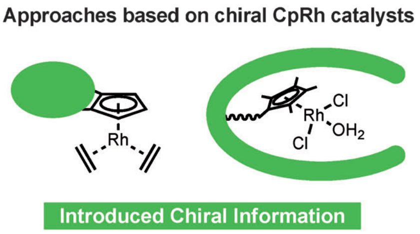

For the USA and Canada:
ANGEWANDTE CHEMIE International Edition (ISSN 1433-7851) is published weekly by Wiley-VCH, PO Box 191161, 69451 Weinheim, Germany. Air freight and mailing in the USA by Publications Expediting Inc., 200 Meacham Ave., Elmont, NY 11003. Periodicals postage paid at Jamaica, NY 11431. US POSTMASTER: send address changes to *Angewandte Chemie*, Journal Customer Services, John Wiley & Sons Inc., 350 Main St., Malden, MA 02148-5020. Annual subscription price for institutions: US$ 11.738/10.206 (valid for print and electronic / print or electronic delivery); for individuals who are personal members of a national chemical society prices are available on request. Postage and handling charges included. All prices are subject to local VAT/sales tax.

Minireviews

Atmospheric Chemistry

T. Salthammer* ______ **3320 – 3327**

Formaldehyde in the Ambient Atmosphere: From an Indoor Pollutant to an Outdoor Pollutant?

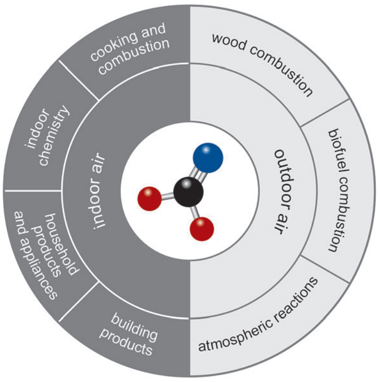

Formaldehyde is a well-known gaseous indoor pollutant. In recent years different countries and organizations have developed concepts for the evaluation of indoor air quality, and consequently, the indoor concentrations of formaldehyde have decreased. However, in the outdoor air in many metropolitan areas, formaldehyde concentrations are continuously growing and sometimes exceed guideline values for indoor air.

Reviews

C–F Activation

M. F. Kuehnel, D. Lentz,*
T. Braun* ______ **3328 – 3348**

Synthesis of Fluorinated Building Blocks by Transition-Metal-Mediated Hydrodefluorination Reactions

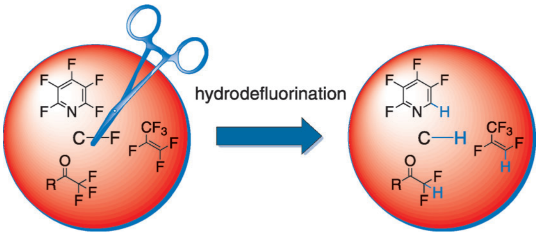

Keen on fluorine: Metal-induced C–F bond activation is emerging as a promising tool to access partly fluorinated molecules (see scheme). Hydrodefluorination has been achieved in the coordination sphere of various transition-metal complexes and features a unique mechanistic diversity.

Communications

Cellular Imaging

VIP

S. Ding, X. Qiao, J. Suryadi, G. S. Marrs,
G. L. Kucera, U. Bierbach* _ **3350 – 3354**

Using Fluorescent Post-Labeling To Probe the Subcellular Localization of DNA-Targeted Platinum Anticancer Agents

Green around the cells: A post-labeling method was developed to image a DNA-targeted platinum drug in cancer cells by confocal fluorescence microscopy. This was done using ligation chemistry between an azide-functionalized platinum-acridine anticancer drug and an alkyne-modified dye, Alexa Fluor 488 (green star, see figure). The platinum-acridine agent was shown to accumulate in the nucleoli of cancer cells (NCI-H460).

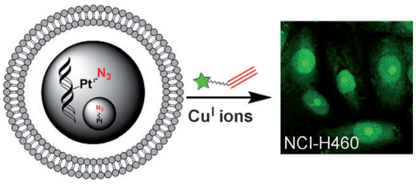

Frontispiece

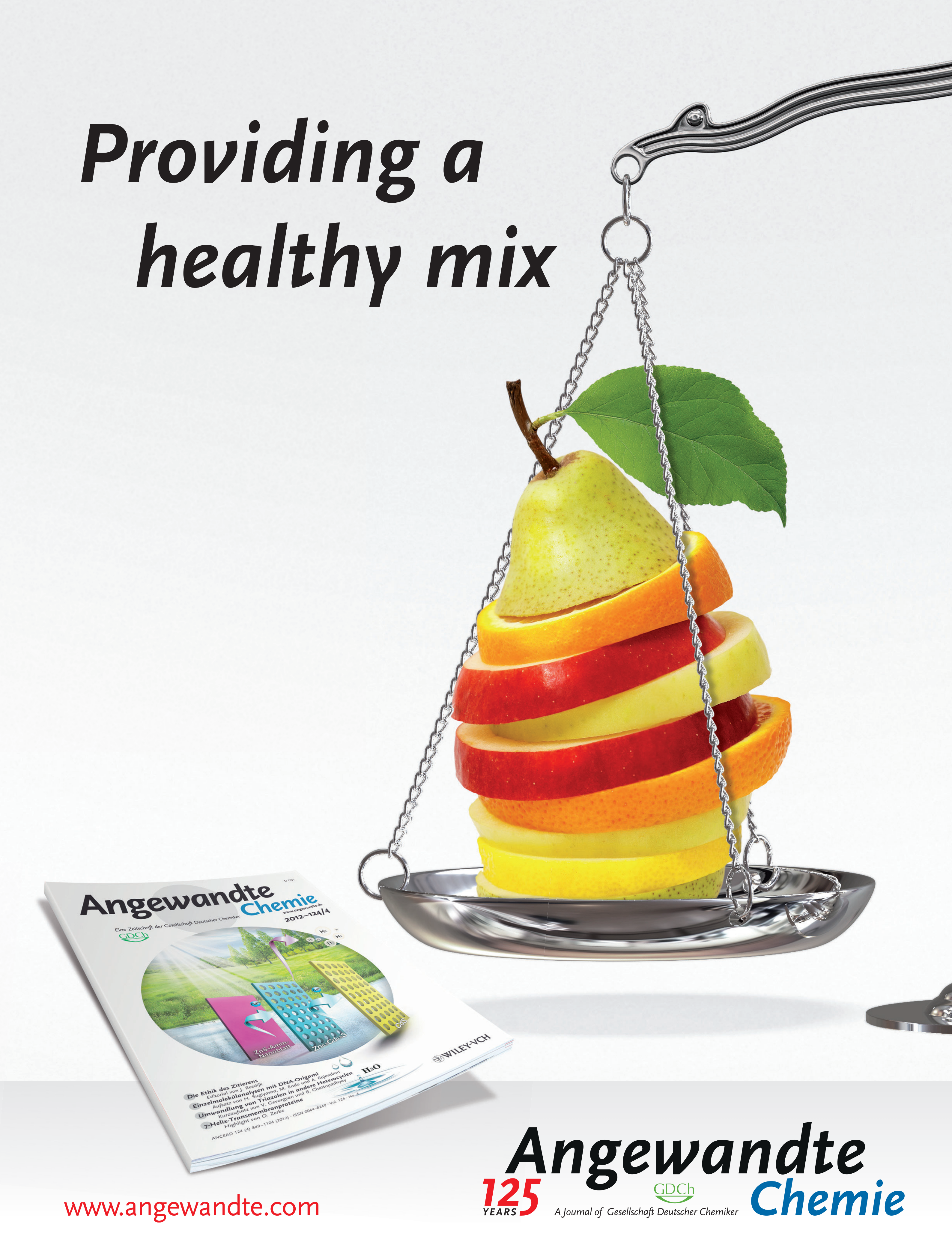
Providing a healthy mix
Angewandte Chemie
Eine Zeitschrift der Gesellschaft Deutscher Chemiker
2012–124/4
ZnS-Amin-Nanoblatt
Zn0.5Cd0.5S
CdS
H2O
WILEY-VCH
Die Ethik des Zitierens
Editorial von J. Reedijk
Einzelmolekülanalysen mit DNA-Origami
Aufsatz von H. Sugiyama, M. Endo und A. Rajendran
Umwandlung von Triazolen in andere Heterocyclen
Kurzaufsatz von V. Gevorgyan und B. Chattopadhyay
7-Helix-Transmembranproteine
Highlight von O. Zerbe
ANCEAD 124 (4) 849–1104 (2012) · ISSN 0044-8249 · Vol. 124 · No. 4
www.angewandte.com
125 YEARS
GDCh
A Journal of Gesellschaft Deutscher Chemiker
Angewandte Chemie

Zeolites

W. Chaikittisilp, Y. Suzuki, R. R. Mukti,
T. Suzuki, K. Sugita, K. Itabashi,
A. Shimojima, T. Okubo* ____ **3355 – 3359**

Formation of Hierarchically Organized Zeolites by Sequential Intergrowth

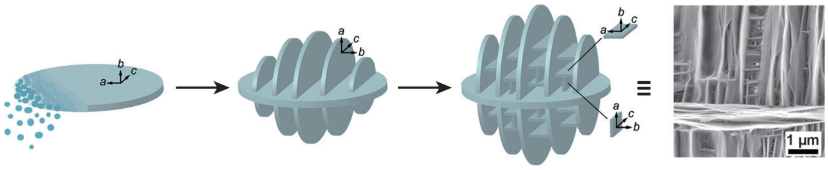

Make intergrowth, not war! Hierarchically organized MFI zeolites with micro-, meso-, and macroporosity (see scheme) in one structure were made by sequential intergrowth by using a simple organic structure-directing agent (OSDA) without meso- or macroporogens. The use of an OSDA that imperfectly fits the zeolite framework generated very thin zeolite plates with 90° rotational intergrowth.

Contracted Porphyrins

D. Kuzuhara, Y. Sakakibara, S. Mori,
T. Okujima, H. Uno,
H. Yamada* ____ **3360 – 3363**

Thiatriphyrin(2.1.1): A Core-Modified Contracted Porphyrin

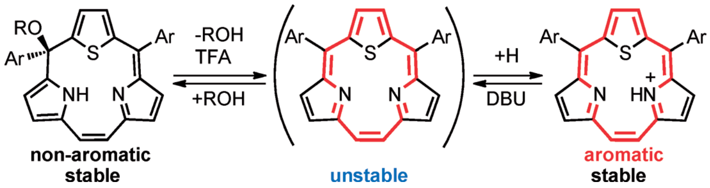

Elusive in its free-base form, the core-modified contracted porphyrin thiatriphyrin(2.1.1) was prepared with *p*-tolyl substituents by intramolecular McMurry coupling and then converted into various alkoxy-substituted analogues (see scheme; DBU = 1,8-diazabicyclo-[5.4.0]undec-7-ene). In the presence of trifluoroacetic acid (TFA), each of these compounds was transformed into the protonated thiatriphyrin(2.1.1), which exhibited moderate aromaticity.

Self-Assembly

VIP

L. Jiang, J. W. J. de Folter, J. Huang,*
A. P. Philipse, W. K. Kegel,
A. V. Petukhov* ____ **3364 – 3368**

Helical Colloidal Sphere Structures through Thermo-Reversible Co-Assembly with Molecular Microtubes

Inside Cover

The co-assembly of spherical colloids and surfactant–cyclodextrin microtubes yields a library of dynamic colloid-in-tube structures, including helices. In situ observations of these structures, including their thermo-reversible assembly and disassembly, demonstrate the potential of the interplay between molecular and colloidal self-assembly, thereby providing a novel route to temperature-sensitive particle alignment and release.

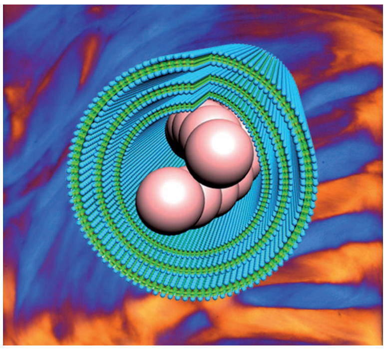

Interface Engineering

J. Wang, Z. Wang, Q. Li, L. Gan, X. Xu,
L. Li,* X. Guo* ____ **3369 – 3373**

Revealing Interface-Assisted Charge-Transfer Mechanisms by Using Silicon Nanowires as Local Probes

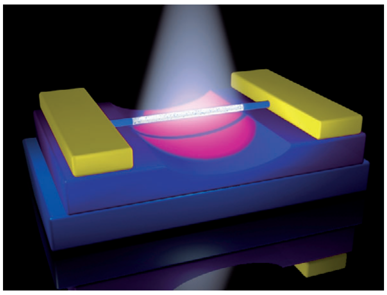

A semiconductor/environment interface has been formed in which suspended silicon nanowires (SiNWs) are in direct contact with photoactive TiO_2 quantum dots. The photoactivity of TiO_2 competes with the intrinsic photoresponses of p-type silicon nanowires. Rational control of the competitive mechanism realizes remarkable mirror-imaging photo-switching and superior rectifying effects in a single SiNW-based device.

Neurochemistry

V. B. Kenche, L. W. Hung, K. Perez, I. Volitakes, G. Ciccotosto, J. Kwok, N. Critch, N. Sherratt, M. Cortes, V. Lal, C. L. Masters, K. Murakami, R. Cappai, P. A. Adlard, K. J. Barnham* **3374 – 3378**

Development of a Platinum Complex as an anti-Amyloid Agent for the Therapy of Alzheimer's Disease

Brainwash! A platinum complex (see scheme) was developed that could be administered orally and reduce the amyloid burden in the brains of transgenic mouse models suffering from Alzheimer's disease. Analyses of brain tissues showed that treatment with the Pt compound led to a 26% decrease in the number of amyloid β-peptide plaques.

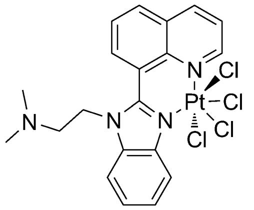

Cancer Diagnosis

S. Hou, L. Zhao, Q. Shen, J. Yu, C. Ng, X. Kong, D. Wu, M. Song, X. Shi, X. Xu, W.-H. OuYang, R. He, X.-Z. Zhao, T. Lee, F. C. Brunicardi, M. A. Garcia,* A. Ribas,* R. S. Lo,* H.-R. Tseng* **3379 – 3383**

Polymer Nanofiber-Embedded Microchips for Detection, Isolation, and Molecular Analysis of Single Circulating Melanoma Cells

Inside Back Cover

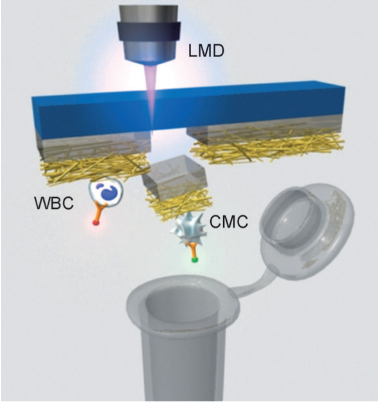

Confined to one cell: A method to detect and isolate single circulating melanoma cells (CMCs; see figure) has been produced by integrating a polymer-nanofiber-embedded nanovelcro cell-affinity assay with a laser microdissection (LMD) technique. This method is able to separate CMCs from normal white blood cells (WBCs) and sequence individual cells for a specific mutation related to cancer progression, allowing for more personalized cancer therapy.

Protein Binding

T. K. Yu, Y. J. Yun, K. O. Lee, J. Y. Suh* **3384 – 3388**

Probing Target Search Pathways during Protein–Protein Association by Rational Mutations Based on Paramagnetic Relaxation Enhancement

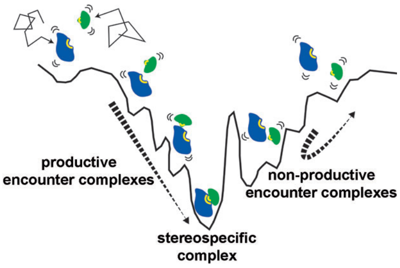

Not just a random encounter: Protein–protein association involves short-lived encounter complexes that can be productive or non-productive according to their roles in the specific complex formation (see scheme). A study of mutant proteins forming a complex based on NMR paramagnetic relaxation enhancement demonstrates that productive encounter complexes can be directly monitored and located quantitatively.

Molecular Spintronics

K. Hong, W. Y. Kim* **3389 – 3393**

Fano-Resonance-Driven Spin-Valve Effect Using Single-Molecule Magnets

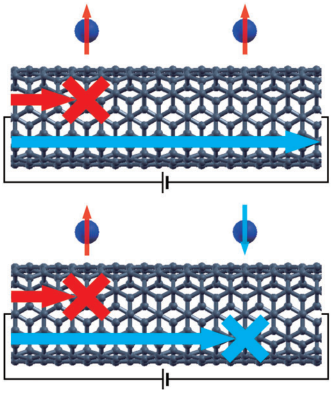

What's your spin on it? A carbon nanotube device decorated with single-molecule magnets through π–π stacking interactions (see scheme) was shown to have spin-dependent transmission (red = spin-up, blue = spin-down) around the energy levels of the molecule owing to Fano resonance, which could be tuned by adjusting the strength of the π–π stacking. This Fano-resonance-driven spin-valve effect offers a new method to make molecular spintronics.

Chiral Surfaces

Y. Yun, A. J. Gellman* ______ **3394 – 3397**

Enantioselective Separation on Naturally Chiral Metal Surfaces: D,L-Aspartic Acid on Cu(3,1,17)$^{R\&S}$ Surfaces

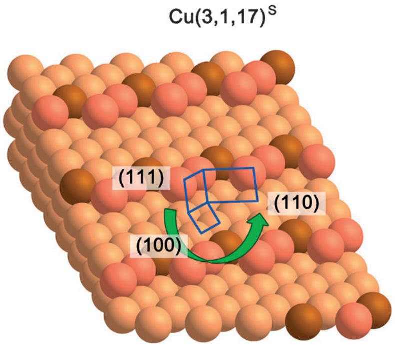

Unequivocal evidence of enantioselective, equilibrium separation of a racemic mixture on a naturally chiral metal surface is presented for the first time. The enantioselectivity is much higher than that of chiral molecules on mineral surfaces. Furthermore, the quantitative nature of the ^{13}C labeling method provides the first direct measure of an enantiospecific adsorption energy difference on a chiral metal surface.

Water Splitting

Y. Jiang, F. Li,* B. Zhang, X. Li, X. Wang, F. Huang, L. Sun* ______ **3398 – 3401**

Promoting the Activity of Catalysts for the Oxidation of Water with Bridged Dinuclear Ruthenium Complexes

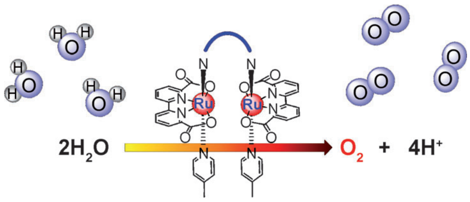

Solar fuels: Dinuclear ruthenium catalysts prepared from two covalently bridged monomeric catalytic units show outstanding activities towards the oxidation of water with high turnover numbers up to 43 000 and turnover frequencies up to 40 s^{-1} (see picture). Direct comparison of the performance parameters indicates that the dimers are significantly more active as catalysts than the monomers.

Adsorption Characteristics

B. Liu, M. Tu, R. A. Fischer* **3402 – 3405**

Metal–Organic Framework Thin Films: Crystallite Orientation Dependent Adsorption

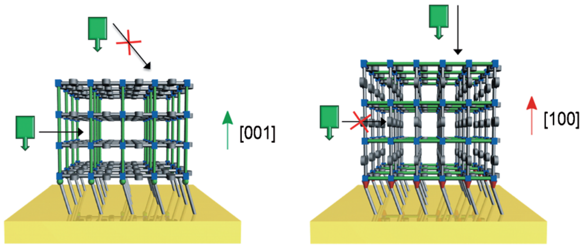

Well oriented: Preferred [100] and [001] orientations of metal–organic framework crystallites, $[Cu_2(ndc)_2(dabco)]$ (ndc = 1,4-naphthalenedicarboxylate, dabco = 1,4-diazabicyclo[2.2.2]octane), attached to surfaces were fabricated. Different pore openings owing to anisotropic properties of $[Cu_2(ndc)_2(dabco)]$ result in oriented thin films exhibiting distinct adsorption kinetics for volatile organic compounds.

Structure–Property Relationship

H. Wu, H. Yu, S. Pan,* Z. Huang, Z. Yang, X. Su, K. R. Poeppelmeier* _ **3406 – 3410**

$Cs_2B_4SiO_9$: A Deep-Ultraviolet Nonlinear Optical Crystal

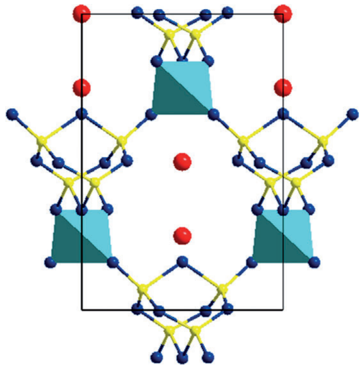

Nonlinear optics: A new borosilicate, $Cs_2B_4SiO_9$, has been synthesized (see picture). This compound represents a new kind of a boron-rich borosilicate and shows a 4.6 times stronger powder second-harmonic generation response relative to KH_2PO_4. In addition, $Cs_2B_4SiO_9$ has a short UV cutoff edge (below 190 nm).

Biomimetic Transfer Hydrogenation

A. McSkimming, M. M. Bhadbhade,
S. B. Colbran* ____________ **3411 – 3416**

Bio-Inspired Catalytic Imine Reduction by Rhodium Complexes with Tethered Hantzsch Pyridinium Groups: Evidence for Direct Hydride Transfer from Dihydropyridine to Metal-Activated Substrate

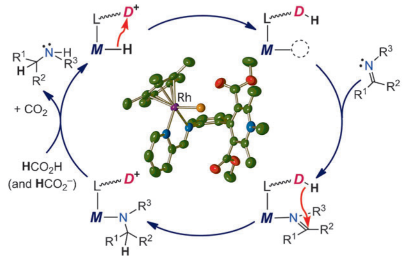

Inspired by Nature: A conceptually new design for a catalyst, combining a metal center abutted to an organic hydride donor, is demonstrated for the formate-driven transfer hydrogenation of imines under ambient conditions. A key step, transfer of hydride from the organohydride donor to the metal-polarized substrate, mirrors that in metallo-(de)hydrogenase enzymes.

Front Cover

Organic Electronic Devices

C. Min, C. Shi, W. Zhang, T. Jiu, J. Chen,*
D. Ma, J. Fang* ____________ **3417 – 3420**

A Small-Molecule Zwitterionic Electrolyte without a π-Delocalized Unit as a Charge-Injection Layer for High-Performance PLEDs

Down to the bare bones: Small-molecule zwitterionic materials were found to be more efficient as charge-injection materials in an organic electronic device than a previously described polymer (see structures). Furthermore, the superior device performance observed for **1** indicates that it is not necessary to focus only on π-delocalized systems and that solid ionic liquids may be promising alternative candidates for charge-injection materials.

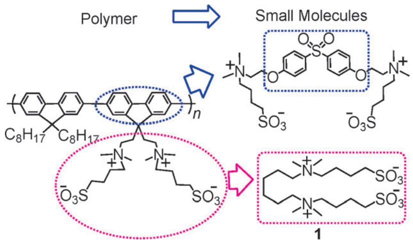

1

Natural Product Synthesis

A. Axelrod, A. M. Eliasen, M. R. Chin,
K. Zlotkowski, D. Siegel* ___ **3421 – 3424**

Syntheses of Xanthofulvin and Vinaxanthone, Natural Products Enabling Spinal Cord Regeneration

Growth promoting: The first synthesis of the natural product xanthofulvin (SM-216289) has resolved issues regarding its structural assignment and that described for the natural product 411J. The structurally and biologically related natural product vinaxanthone was similarly prepared through a novel dimerization reaction. Treatment of *C. elegans* with synthetic xanthofulvin and vinaxanthone enhanced axonal branching.

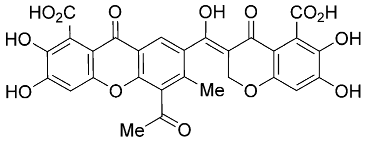

xanthofulvin

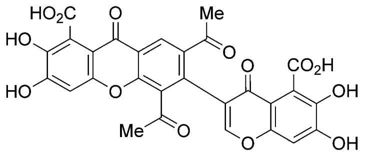

vinaxanthone

PELDOR Spectroscopy

P. E. Spindler, S. J. Glaser, T. E. Skinner,
T. F. Prisner* ____________ **3425 – 3429**

Broadband Inversion PELDOR Spectroscopy with Partially Adiabatic Shaped Pulses

Distance and spins: A new broadband, frequency-selective inversion pulse has been devised for pulsed electron–electron double resonance (PELDOR) spectroscopy, a unique method used to determine distance distributions between two or more paramagnetic centers 2–10 nm apart. The PELDOR modulation depth can be increased by substituting the rectangular pump pulse by a shaped pulse.

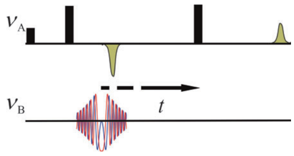

Uranium magnets: Three uranium(III) complexes with distinctly different structures and compositions are all shown to display slow relaxation of the magnetization. This study greatly expands the range of slowly relaxing uranium complexes, and demonstrates that this behavior is not limited to specific ligand types or molecular symmetries (see picture).

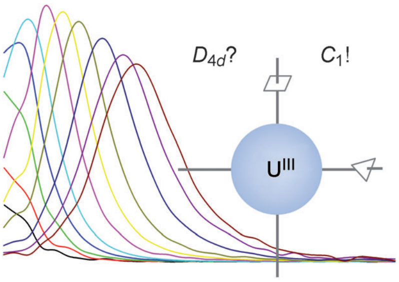

Single-Molecule Magnets

F. Moro, D. P. Mills, S. T. Liddle,* J. van Slageren* ———— **3430–3433**

The Inherent Single-Molecule Magnet Character of Trivalent Uranium

---

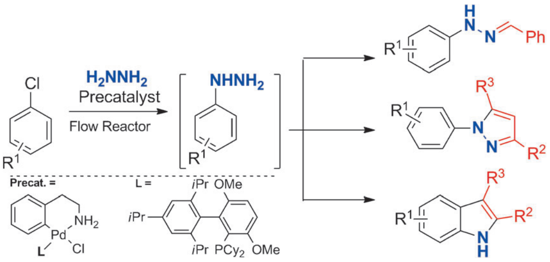

Minimizing risk: The synthesis of arylhydrazines through C–N cross-coupling of aryl chlorides with hydrazine is described. Through the use of continuous flow, the hazards associated with the use of hydrazine in the presence of transition metals are decreased. In addition, multistep flow sequences have also been developed for the generation of functionalized heterocycles utilizing the arylhydrazine intermediates.

Cross-Coupling

A. DeAngelis, D.-H. Wang, S. L. Buchwald* ———— **3434–3437**

Mild and Rapid Pd-Catalyzed Cross-Coupling with Hydrazine in Continuous Flow: Application to the Synthesis of Functionalized Heterocycles

---

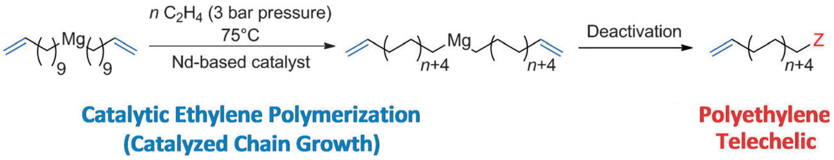

A functional chain transfer agent, bis(10-undecenyl)magnesium, was employed as cocatalyst in conjunction with $[(C_5Me_5)_2NdCl_2Li(OEt_2)_2]$ to catalyze polyethylene (PE) chain growth on magnesium. Vinyl-PE-Mg-PE-vinyl units were then further functionalized. This is the first example of catalytic ethylene polymerization with single-step, in situ functionalization to telechelic polyethylenes.

Telechelic Polyethylene

I. German, W. Kelhifi, S. Norsic, C. Boisson,* F. D'Agosto* ———— **3438–3441**

Telechelic Polyethylene from Catalyzed Chain-Growth Polymerization

---

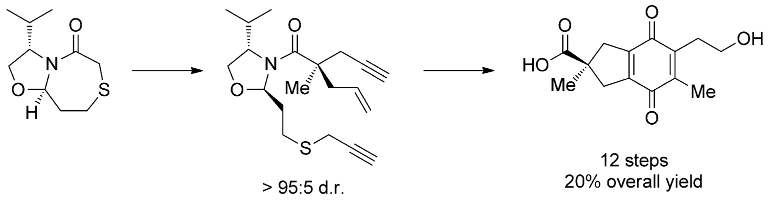

Distant relative: The configuration of the quaternary stereocenter in puraquinonic acid (see scheme, right) is defined by groups far removed from the point of asymmetry. The use of a bicyclic thioglycolate lactam to set the quaternary stereocenter at an early stage cuts the length of the synthesis of the natural product by nearly two thirds.

Natural Product Synthesis

E. A. Tiong, D. Rivalti, B. M. Williams, J. L. Gleason* ———— **3442–3445**

A Concise Total Synthesis of (*R*)-Puraquinonic Acid

Medicinal Chemistry

L. Chen, K. B. Riaz Ahmed, P. Huang, Z. Jin* **3446 – 3449**

Design, Synthesis, and Biological Evaluation of Truncated Superstolide A

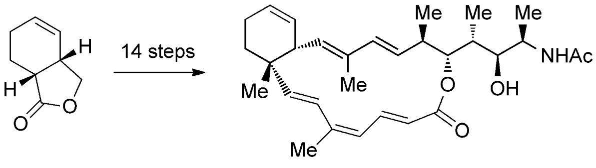

Truncated superstolide A

By design: A truncated superstolide A, a simplified analogue of the potent anticancer marine macrolide superstolide A, was designed and successfully synthesized by a highly efficient and convergent approach. The biological evaluation showed that this compound maintains the potent anticancer activity of the original natural product superstolide A.

Asymmetric Reactions

Y. Hayashi,* S. Umemiya **3450 – 3452**

Pot Economy in the Synthesis of Prostaglandin A_1 and E_1 Methyl Esters

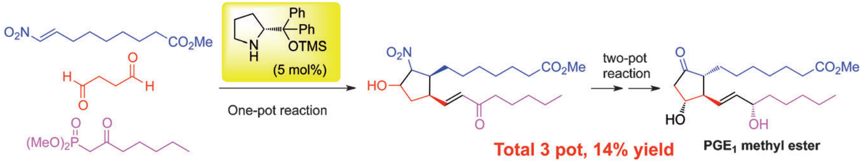

Pot luck: Prostaglandins regulate a broad range of physiological processes and some of their derivatives are used as effective drugs, but previously their preparation has required many steps. The title compounds were efficiently synthesized in a small number of synthetic steps by using a recently developed organocatalyst and practical, one-pot operations involving several successive reactions.

Surface Chemistry

A. D. Gordon, F. Zaera* **3453 – 3456**

Adsorption of 1-(1-Naphthyl)ethylamine from Solution onto Platinum Surfaces: Implications for the Chiral Modification of Heterogeneous Catalysts

Chiral modification of catalysts: A comparative in situ reflection–absorption infrared spectroscopy study of the adsorption of 1-(1-naphthyl)ethylamine on Pt surfaces from solution indicated bonding mainly through the amine group and not the aromatic ring as commonly assumed (see picture). In light of these results, a rethinking of the existing model for chiral modification of catalysts may be needed.

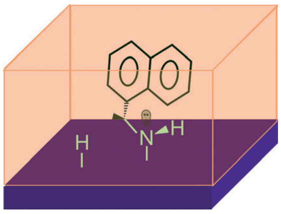

Synthetic Methods

X. Shao, X.-Q. Wang, T. Yang, L. Lu,* Q. Shen* **3457 – 3460**

An Electrophilic Hypervalent Iodine Reagent for Trifluoromethylthiolation

Back Cover

Sulfur and friends: A new electrophilic hypervalent iodine reagent **1** has been developed for direct trifluoromethylthiolation. A variety of nucleophiles, including β-ketoesters, aldehydes, amides, aryl or vinyl boronic acids, and alkynes, reacted with **1** under mild conditions to give the corresponding trifluoromethylthiolated compounds in good to excellent yields.

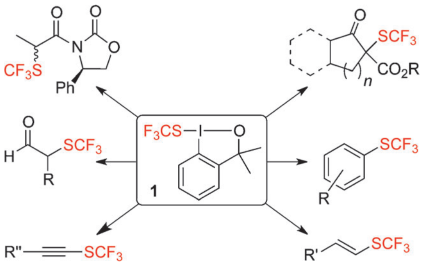

Asymmetric Catalysis

Y. Shimoda, T. Kubo, M. Sugiura, S. Kotani,* M. Nakajima* **3461 – 3464**

Stereoselective Synthesis of Multiple Stereocenters by Using a Double Aldol Reaction

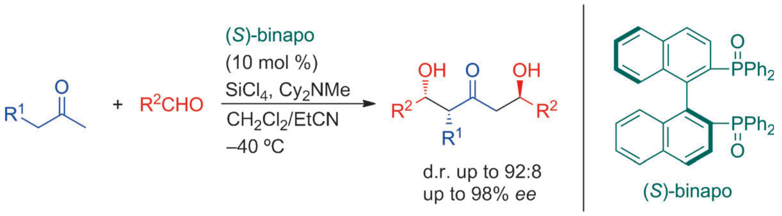

Triple play: The title reaction of an alkyl methyl ketone and two aldehydes using chiral (*S*)-binapo as a Lewis base catalyst allows access to 1,5-dihydroxy-3-pentanone derivatives with multiple chiral centers in good yields with high diastereo- and enantioselectivities in a single operation (see scheme).

Heterogeneous Catalysis

S. Guo, D. Li, H. Zhu, S. Zhang, N. M. Markovic, V. R. Stamenkovic,* S. Sun* **3465 – 3468**

FePt and CoPt Nanowires as Efficient Catalysts for the Oxygen Reduction Reaction

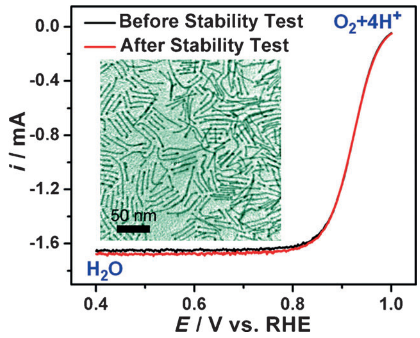

Pt alloy nanowires (NWs) were synthesized and applied as catalysts in the title reaction. The specific activity and mass activity of 2.5 nm wide FePt NWs (see TEM picture) were higher than those of a commercial Pt catalyst. The stability of FePt NWs was tested by scanning the potential in an O$_2$-saturated HClO$_4$ solution. The corresponding polarization curves before and after the test (see picture) indicate that these NWs are robust catalysts.

Germanium(II) Adducts

R. Bandyopadhyay, J. H. Nguyen, A. Swidan, C. L. B. Macdonald* **3469 – 3472**

Water and Ammonia Complexes of Germanium(II) Dications

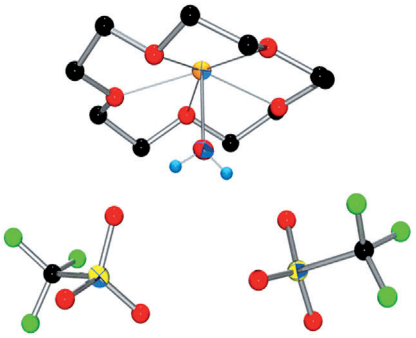

Craftily crowned: The treatment of crown ether Ge^{II} dications with water or ammonia produces the stable complexes [([15]crown-5)Ge·OH$_2$][OTf]$_2$ (see picture; Ge orange, O red, F green, S yellow, H blue) and [([15]crown-5)Ge·NH$_3$][OTf]$_2$. The OH and NH hydrogen atoms are rendered more acidic in these compounds.

Asymmetric Catalysis

J. N. Zhao, X. H. Liu, W. W. Luo, M. S. Xie, L. L. Lin, X. M. Feng* **3473 – 3477**

Asymmetric Synthesis of β-Amino Nitriles through a Sc^{III}-Catalyzed Three-Component Mannich Reaction of Silyl Ketene Imines

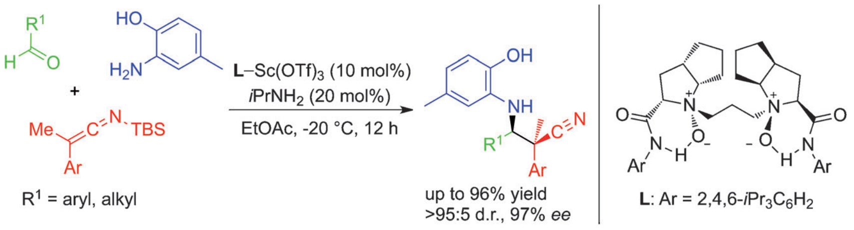

A range of β-amino nitriles containing contiguous tertiary and quaternary stereogenic carbon centers were synthesized by using the title reaction. The reaction was catalyzed by a chiral *N*,*N*′-dioxide scandium(III) complex under mild reaction conditions. Based on experimental investigations, a possible transition state has been proposed to explain the origin of asymmetric inductivity.

Cross-Coupling

L. Wang, H. Huang, D. L. Priebbenow, F.-F. Pan, C. Bolm* ———— **3478 – 3480**

Copper-Catalyzed Oxidative Cross-Coupling of Sulfoximines and Alkynes

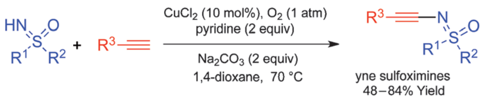

A 'Cu'te couple: A synthetically useful protocol for the preparation of N-alkynylated sulfoximines (yne sulfoximines) has been developed. The method involves a mild copper-catalyzed oxidative cross-coupling of NH-sulfoximines and terminal alkynes (see scheme). The corresponding N-acyl sulfoximines were also obtained selectively after acid-catalyzed hydrolysis of the yne sulfoximines.

Cage Compounds

N. S. Townsend, S. R. Shadbolt, M. Green, C. A. Russell* ———— **3481 – 3484**

Phosphacycles as Building Blocks for Main Group Cages

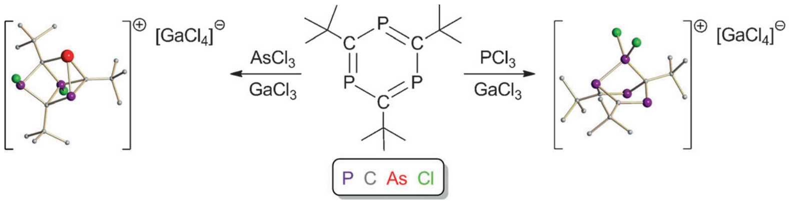

Cationic pnictogen/carbon cages are formed from reaction of 2,4,6-tri-*tert*-butyl-1,3,5-triphosphabenzene with the carbene mimics EX_2^+ (E = P, As). For E = P, 1,4-addition to the hetereoaromatic compound is observed, whereas for E = As, cage complexes are formed.

Cycloaddition

S. Zhang, W.-X. Zhang, Z. Xi* ———— **3485 – 3489**

Lewis Acid Catalyzed Site-Selective Cycloadditions of 2,6-Diaza-semibullvalenes with Isocyanides, Azides, and Diazo Compounds for the Synthesis of Diaza- and Triazabrexadiene Derivatives

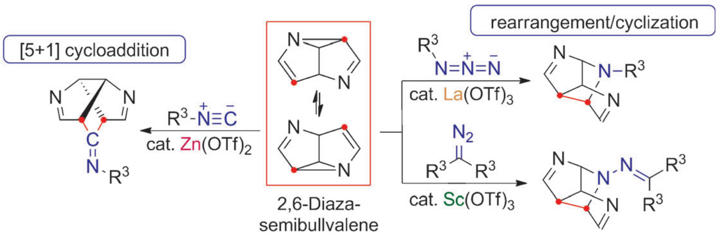

Unprecedented cycloaddition pathways: Lewis acid catalyzed cycloadditions of 2,6-diazasemibullvalenes with isocyanides, azides, and diazo compounds lead to structurally interesting and otherwise unavailable cage diaza- and triazabrexadiene derivatives. Unique rearrangement/cycloaddition pathways are revealed.

Asymmetric Organocatalysis

I. Čorić, J. H. Kim, T. Vlaar, M. Patil, W. Thiel, B. List* ———— **3490 – 3493**

Brønsted Acid Catalyzed Asymmetric S_N2-Type O-Alkylations

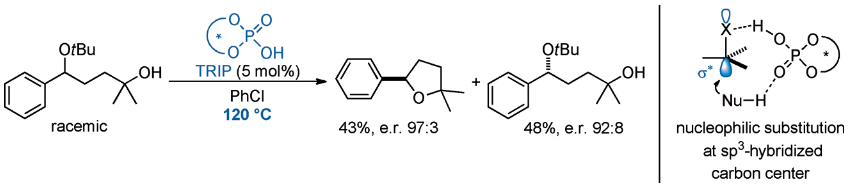

Bridging the gap: Brønsted acids catalyze an intramolecular S_N2-type alkylation of alcohols with ethers by bridging a pentacoordinate transition state, thus simultaneously activating both the leaving group and nucleophile (see scheme). Density functional calculations provide detailed insight into the course of the reaction and the transition-state structure.

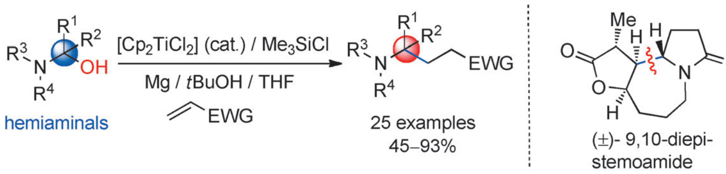

Radical measures: A radical coupling reaction, which is proposed to proceed through in situ chlorination of a hydroxy group by Me_3SiCl, is used to form quaternary carbon centers with amino groups in α position. The reaction can be scaled up and is used in an efficient six-step total synthesis of (±)-9,10-diepi-stemoamide (see scheme, Cp = cyclopentadienyl, EWG = electron-withdrawing group).

Radical Reactions

X. Zheng,* X.-J. Dai, H.-Q. Yuan, C.-X. Ye, J. Ma, P.-Q. Huang ______ **3494 – 3498**

Umpolung of Hemiaminals: Titanocene-Catalyzed Dehydroxylative Radical Coupling Reactions with Activated Alkenes

---

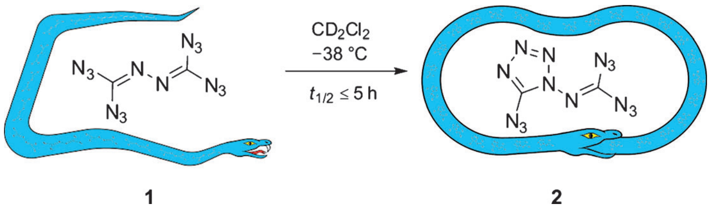

Rapid ring closure transforms the tetraazide **1**, which was thought to have been characterized at room temperature in 1961 and 2009, into the tetrazole **2**. Consequently, the previously synthesized compounds actually are identical with heterocycle **2**, which was also prepared by a third method in 2011. After its generation at low temperature, the open-chain compound **1** and its cyclization reaction have now been analyzed for the first time.

Binary CN Compounds

K. Banert,* S. Richter, D. Schaarschmidt, H. Lang ______ **3499 – 3502**

Well Known or New? Synthesis and Structure Assignment of Binary C_2N_{14} Compounds Reinvestigated

---

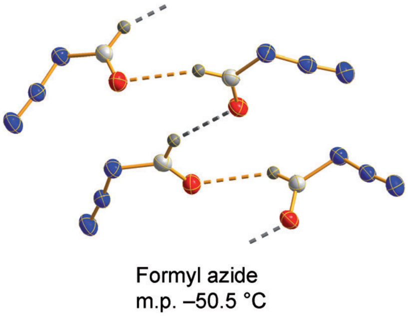

The simplest acyl azide, $HC(O)N_3$, has been prepared as the neat substance and characterized by IR and Raman spectroscopy and low-temperature X-ray crystallography (see solid-state structure; C white, H gray, N blue, O red). Photolysis of the azide in CO-doped solid noble-gas matrices furnished the first experimental proof of the elusive parent acyl isocyanate HC(O)NCO.

Covalent Azides

X. Zeng,* E. Bernhardt, H. Beckers,* K. Banert, M. Hagedorn, H. Liu ______ **3503 – 3506**

Formyl Azide: Properties and Solid-State Structure

Grignard deluxe: The 1,2-dimethoxyethane adduct of phenylcalcium iodide forms the unique solvent-separated species $[(dme)_3CaPh]^+I^-$ with a highly Lewis acidic metal center. Degradation of DME occurs, yielding calcium methoxide cages, such as $[\{(dme)Ca\}_4(CaI)_2(\mu_3\text{-}OMe)_8(\mu_6\text{-}O)]$, and methyl vinyl ether. The picture shows the crystal structure of $[(dme)_3CaPh]^+$ (Ca brown, C gray, O red).

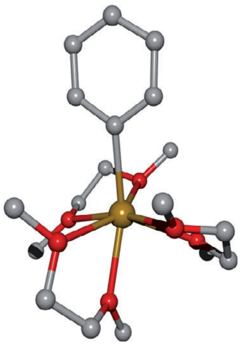

Organocalcium Compounds

J. Langer, M. Köhler, J. Hildebrand, R. Fischer, H. Görls, M. Westerhausen* ______ **3507 – 3510**

Stabilization and Reactivity of the Lewis Acidic Solvated Phenylcalcium Cation

Aggregation Inhibitors

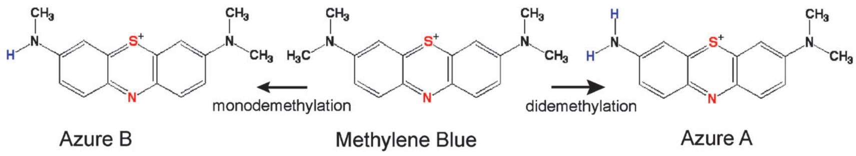

Blues brothers: Aggregation of the Tau protein is a key event in Alzheimer's disease and Tau aggregation inhibitors are important as potential drugs. Phenothiazines, such as methylene blue and its azure derivatives, have a unique mechanism, specifically modifying the Tau cysteine residues. The modification keeps Tau in a monomeric disordered conformation preventing the formation of filaments and their toxic precursors.

Silicon Double Bonds

There and back: An isocyanide-centered silene–disilene reversibility was observed for the insertion of isocyanides into unsymmetrically substituted disilenes. This reaction leads to the formation of silenes at room temperature; the disilene is regenerated in the presence of a Lewis acid.

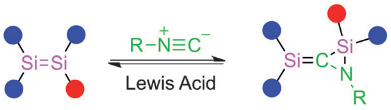

Fullerene Chemistry

The ins and outs of fullerene chemistry: Fullerenophosphates with a C_3-symmetrical *e*,*e*,*e*-trisaddition pattern were synthesized with high regioselectivity. *In*- (see structure, red O, yellow P, blue C) and *out*-invertomers, based on the orientation of the P=O group, were isolated and their structures were confirmed by X-ray-crystallography.

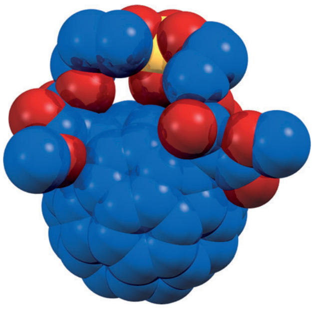

NMR Spectroscopy of Proteins

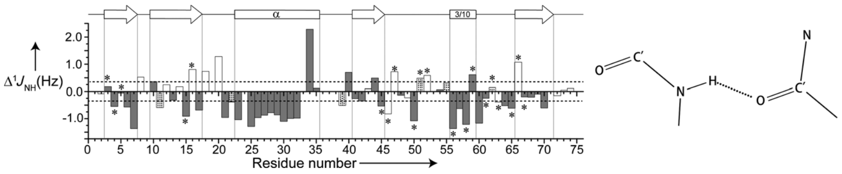

Sensitive information: Hydrogen bonds stabilize protein structures and are critical for many chemical and biological phenomena. NMR studies found that the one-bond $^1H–^{15}N$ scalar coupling constant is increased by up to 1.6 Hz when a hydrogen bond is formed. These coupling constants therefore provide a sensitive tool for studying protein structure.

Golden beauty: For the first time a ligand-stabilized Au$_{14}$ cluster has been examined. The structure of this superatom complex bears several impressive and unique features, which will further support the understanding of certain guiding principles for molecular-precision synthesis and functionalization of ultrasmall nanoparticles.

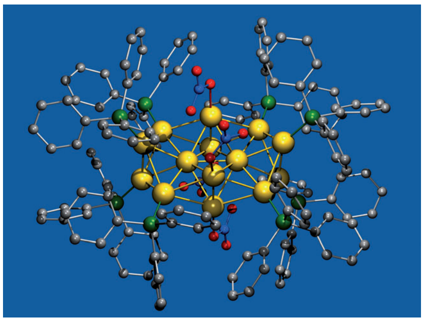

Ligand-Stabilized Gold Clusters

B. S. Gutrath, I. M. Oppel, O. Presly, I. Beljakov, V. Meded, W. Wenzel, U. Simon* ______________ **3529–3532**

$[Au_{14}(PPh_3)_8(NO_3)_4]$: An Example of a New Class of Au(NO$_3$)-Ligated Superatom Complexes

---

Supporting information is available on www.angewandte.org (see article for access details).

A video clip is available as Supporting Information on www.angewandte.org (see article for access details).

This article is available online free of charge (Open Access).

This article is accompanied by a cover picture (front or back cover, and inside or outside).

Angewandte Corrigendum

In this Communication, the incorrect G2 enthalpy data "−56.944771 (See Table S2 in Supporting Information)" of the NH$_4^+$ cation was used for the calculation of the heat of formation of the 2,2-dialkyltriazanium cation. The correct value is "−56.777599." This mistake was caused by an error during input of "Charge" and "Multiplicity" for the G2 calculation of the NH$_4^+$ cation. The correct values are "Charge = 1; Multiplicity = 1"; however, in the original manuscript "Charge = 0; Multiplicity = 2" was used.

As a result, the $\Delta H_{f,\,\text{cation}}$, ΔH_f, P, vD, and I_{sp} data for salts **1** to **7** in Table 1 as published are incorrect. The correct data are given here in Table 1.

The sentence "All of the 2,2-dimethyl triazanium salts have positive heats of formation with **6** the highest (905 kJ mol^{-1}, Table 1)" on page 2794, left column, must be replaced with "Five 2,2-dimethyl triazanium salts have positive heats of formation with **6** the highest (465.4 kJ mol^{-1}, Table 1)."

All other results and conclusions of this Communication remain unaffected. The authors regret any confusion that may have arisen from the erroneous calculation.

Hypergolic Ionic Liquids with the 2,2-Dialkyltriazanium Cation

H. Gao, Y.-H. Joo, B. Twamley, Z. Zhou,* J. M. Shreeve* ______________ **2792–2795**

Angew. Chem. Int. Ed. **2009**, *48*

DOI: 10.1002/anie.200900094

Table 1: Properties of energetic 2,2-dimethyltriazanium salts.[a]

Salts	d[b]	T_m[c]	T_d[d]	Ignition delay[e] N$_2$O$_4$	WFNA	Lattice energy[f]	ΔH_f[f] cation	ΔH_f[f] anion	ΔH_f[f]	P[g]	vD[h]	I_{sp}[i]	IS[j]
1[k]	1.47	–	–	26	nh[l]	576.7	756.8	−230.3	−50.2	–	–	–	>60
2	1.26	−0.19	145.7	8	16	501.2	756.8	−27.1	228.5	16.0	7169	226	>60
3	1.15	10.7	134.2	sh[m]	22[l]	506.5	756.8	113.4	363.7	12.1	6516	201	>60
4	1.48	–	134.2	nh[l]	nh[l]	490.9	756.8	−127.7	138.2	21.2	7644	227	>60
5	1.35	47.8	142.5	nh[l]	nh[l]	492.2	756.8	32.2	296.8	15.5	7009	211	>60
6	1.20	74.4	153.3	nh[l]	nh[l]	491.7	756.8	200.3	465.4	11.1	6207	190	>60
7	1.47	99.0	145.6	10	4	544.5	756.8	−307.9	−95.6	22.2	8034	228	>60
IL A[n]	1.25	−61	–	–	15	481.4	908.0	113.4	540	8.9	5721	186.7	–
IL B[o]	1.41[p]	−66	–	–	31	525.8	895.6	113.4	483	16.2	7158	213.3	–

[a] The P, vD, and I_{sp} values of salts **2** to **7** were calculated using Cheetah 6.0 instead of Cheetah 5.0. [b] Density [g cm^{-3}]. [c] Melting point [°C] (from DSC measurement with b = 10 °C min^{-1}). [d] Decomposition temperature [°C], DSC onsets from measurement with b = 108 °C min^{-1}). [e] [ms]. [f] Heat of formation [kJ mol^{-1}]. [g] Detonation pressure [GPa]. [h] Detonation velocity [m s^{-1}]. [i] Specific impulse measured in seconds (additional information). [j] Impact sensitivity [J] (BAM Fallhammer). [k] The Cheetah calculation for salt **1** failed. [l] nh = not hypergolic. [m] Hypergolic when a second drop of fuel was dropped into N$_2$O$_4$. [n] 1-(2-Pentynyl)-3-methylimidazolium dicyanamide (ref. [3]). [o] 1-Methyl-4-amino-1,2,4-triazolium dicyanamide (ref. [3]). [p] Calculated (ref. [5f]).